Hydrophobicity of Proteins and Interfaces: Insights from Density Fluctuations

Sumanth N. Jamadagni,[1,2] Rahul Godawat,[1,3] and Shekhar Garde[1]

[1]The Howard P. Isermann Department of Chemical and Biological Engineering and the Center for Biotechnology and Interdisciplinary Studies, Rensselaer Polytechnic Institute, Troy, New York 12180; email: jamadagni.sn@pg.com, rahul.godawat@genzyme.com, gardes@rpi.edu

[2]Beckett Ridge Technical Center, The Procter and Gamble Company, West Chester, Ohio 45069

[3]Genzyme Corporation, Framingham, Massachusetts 01701

Annu. Rev. Chem. Biomol. Eng. 2011. 2:147–71

First published online as a Review in Advance on February 18, 2011

The *Annual Review of Chemical and Biomolecular Engineering* is online at chembioeng.annualreviews.org

This article's doi: 10.1146/annurev-chembioeng-061010-114156

1947-5438/11/0715-0147$20.00

Keywords

water structure, hydrophobic interactions, hydrophilicity, protein hydration, heterogeneous surfaces, wetting and adhesion

Abstract

Macroscopic characterizations of hydrophobicity (e.g., contact angle measurements) do not extend to the surfaces of proteins and nanoparticles. Molecular measures of hydrophobicity of such surfaces need to account for the behavior of hydration water. Theory and state-of-the-art simulations suggest that water density fluctuations provide such a measure; fluctuations are enhanced near hydrophobic surfaces and quenched with increasing surface hydrophilicity. Fluctuations affect conformational equilibria and dynamics of molecules at interfaces. Enhanced fluctuations are reflected in enhanced cavity formation, more favorable binding of hydrophobic solutes, increased compressibility of hydration water, and enhanced water-water correlations at hydrophobic surfaces. These density fluctuation–based measures can be used to develop practical methods to map the hydrophobicity/philicity of heterogeneous surfaces including those of proteins. They highlight that the hydrophobicity of a group is context dependent and is significantly affected by its environment (e.g., chemistry and topography) and especially by confinement. The ability to include information about hydration water in mapping hydrophobicity is expected to significantly impact our understanding of protein-protein interactions as well as improve drug design and discovery methods and bioseparation processes.

INTRODUCTION

Some of the common manifestations of hydrophobic effects are the immiscibility of oil and water, low solubility of nonpolar gases in water, and beading up of water on Teflon-coated surfaces. It is now well appreciated that in aqueous environments hydrophobic interactions are one of the key drivers of many biological self-assembly processes, including protein folding, misfolding and aggregation, micelle and membrane formation, and molecular recognition (1–4). This realization stemmed originally from the remarkable similarity in the thermodynamics of transfer of nonpolar solutes into water and that of protein unfolding (1, 5) and created an enormous interest in understanding hydrophobic effects from a molecular perspective. Following the seminal theoretical work by Pratt & Chandler in 1977 (6), molecular theory and simulations initially focused on understanding of primitive hydrophobic effects, namely the solvation of small spherical solutes in water and the water-mediated interactions between them (7–11).

Over the past two decades, many dimensions of this problem have been explored, and hydrophobicity has emerged as a multidimensional challenge for theory, simulations, and experiments (see **Figure 1**). Studies on the effects of various thermodynamic variables such as temperature (10, 12–16), pressure (17–19), and additives—salts (20–23), osmolytes (24, 25), stabilizers, and denaturants (26–31)—on hydrophobic interactions in model systems have revealed a close correspondence with the thermodynamics of biological self-assembly. This has resulted in a sustained interest in understanding the many aspects of hydrophobicity.

From a fundamental perspective, the length-scale dependency of hydrophobicity is one of its most fascinating aspects (32–35). Small and large solutes display remarkably different hydration behavior. Although this phenomenon is not unique to water (36–38), arguably the effect is seen most clearly for water because of its self-associating nature and the resulting large surface tension. Small idealized hydrophobic solutes—hard spheres—are accommodated in the hydrogen-bonded

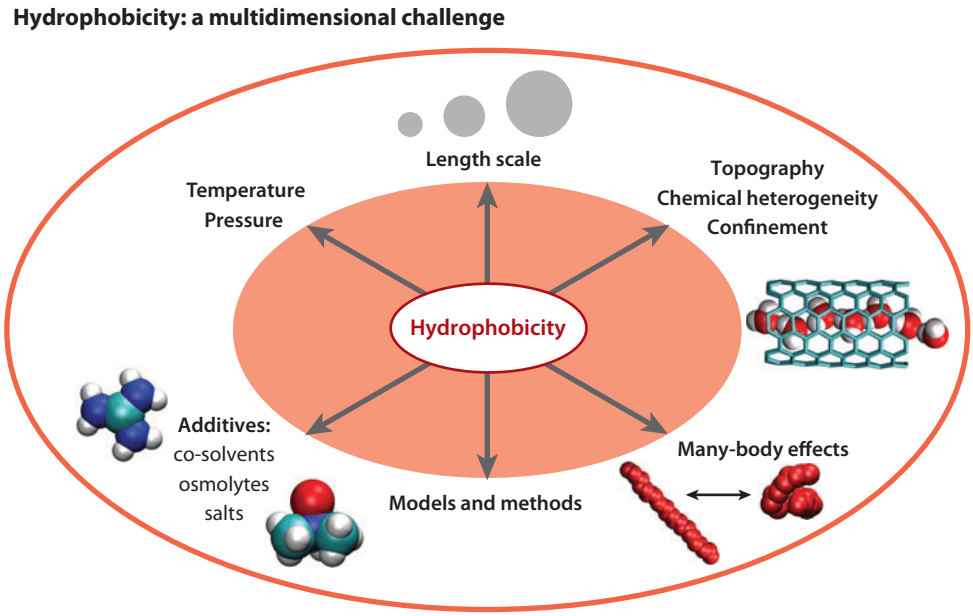

Figure 1

A schematic highlighting the multidimensional nature of the challenge in understanding hydrophobicity.

network of water with negligible perturbation and little or no enthalpic cost, but a large entropic one. Hydration of such solutes is characterized by the statistics of cavity formation or density fluctuations in bulk water (39). As the solute size increases, water molecules can no longer maintain their hydrogen-bonded network around the solute (34). Water thus dewets from the surfaces of large solutes, which creates an interface that for hard-sphere solutes resembles a vapor-liquid interface of water (32, 34). The gradual crossover in hydrophobic hydration with increasing solute size is thus characterized by dewetting of the solute surface, a change in the hydration thermodynamics from entropy to enthalpy dominated, and a change in the physics of hydration from one dominated by spontaneous, molecular-scale fluctuations to one dominated by interface formation.

Elegant theory by Lum, Chandler, & Weeks (LCW) (33) provided a unified description of the length-scale dependency of hydrophobicity and its consequences for the thermodynamics of self-assembly (16, 40). Molecular simulations have confirmed that the gradual crossover from small to large solute hydration behavior begins at nanoscopic length scales (35, 41, 42) and have pointed to an intriguing connection between the crossover and the Egelstaff-Widom length scale in liquids (41, 43). The nanoscopic nature of the crossover length scale implies that both small and large solute hydration thermodynamics play a role in many biological self-assembly processes that occur around this length scale.

Despite these advances, many challenges remain in obtaining a molecular-level understanding and characterization of the hydration of realistic interfaces, especially those containing chemical and/or topographical heterogeneities. To this end, significant strides have been made recently to translate fundamental understanding from model systems to applications to complex heterogeneous surfaces of proteins and nanoparticles (44–54). In this review, we focus on these advances that connect molecular and nanoscale phenomena to their macroscopic manifestations, and specifically those that connect the behavior of water at interfaces to macroscopic measures of hydrophobicity. We anticipate that this review will motivate experiments that can directly test some of the key ideas underlying the conceptual framework presented here.

Finally, in addition to hydrophobicity, other measures exist to quantify the strength of interfacial coupling (e.g., hydrodynamic or thermal). Recent simulation studies and experiments indicate strong connections between these different measures. Understanding these connections will require development of new theories that will lead to deeper insights into these interfacial phenomena.

CHARACTERIZING HYDROPHOBICITY AT THE NANOSCALE

Density Fluctuations as a Signature of Hydrophobicity

Large interfaces with low curvature lie at one end of the length-scale spectrum discussed above. Macroscopically, hydrophobicity of such interfaces is characterized easily by measuring the contact angle of a water droplet placed on the surface (55, 56). Such measurements are not feasible, however, on interfaces of proteins or nanoparticles. Difficulties in defining and characterizing hydrophobicity in such cases have been articulated in a recent perspective article in *Science* by Granick & Bae (57). To this end, a molecular characterization based on the behavior of water at interfaces is needed that will be generally applicable over a range of length scales, chemistries, topographies, and heterogeneities.

Theory as well as simulations show that water dewets and forms a vapor-liquid-like interface near large idealized solutes or near interfaces that interact with water via repulsive interactions (32, 33). This might suggest the local density of water (or the extent of its depletion) to be a convenient molecular measure of hydrophobicity. Realistic interfaces, however, always exert

some attractive (dispersive) interactions on water. Furthermore, they are rarely atomically flat. How different then is the above description near realistic interfaces? And specifically, how does the water phase respond to varying degrees of surface hydrophobicity (quantified macroscopically through straightforward contact angle measurements)?

Experimentalists have used an array of techniques, such as X-ray (58–62) and neutron scattering (63–66), ellipsometry (67), and thermal conductivity (68), to probe aqueous interfaces. Although a consensus appears to be emerging (57, 58, 61, 62, 68) that the width of the depletion region near realistic hydrophobic surfaces is small, less than the size of a water molecule, contradictory experimental data continue to appear that report the width to be as large as 10 Å (69). One origin of the difficulty in measuring the water density profile in the subnanoscopic vicinity of an interface is simply the resolution of current experiments. However, based on theoretical understanding (34) and state-of-the-art simulation data (44), we argue that the density of water near a realistic interface constitutes a poor molecular measure of its hydrophobicity.

Molecular dynamics (MD) simulations of the hydration of interfaces spanning a range of hydrophobicity demonstrate this point clearly (44). **Figure 2** shows water density profiles normal to surfaces of self-assembled monolayers (SAMs) with solvent-exposed head groups ranging from hydrophobic (-CF_3 and -CH_3) to hydrophilic (-OH and -$CONH_2$). Placing nanodroplets of water on these surfaces in independent simulations confirmed that, as expected, the surfaces do span a broad range of hydrophobicity with water droplets beading up on the -CF_3 and -CH_3 SAMs and spreading on the -OH and -$CONH_2$ surfaces (70). In contrast, density profiles in almost all cases

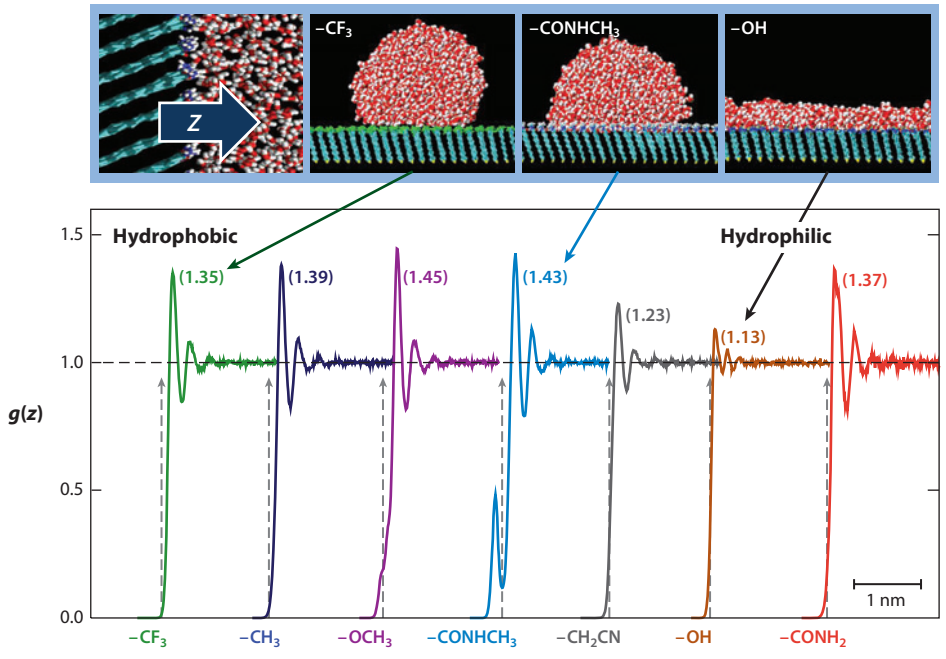

Figure 2

Density profiles of water normal to self-assembled monolayers spanning a range of hydrophobicity (44). Water molecules layer next to all surfaces, and various measures of vicinal density (e.g., height of the first peak, interface width) display little correlation with the hydrophobicity of the surfaces, although independent simulations (70) show that the contact angle of water on these surfaces closely tracks experimental measurements.

show layering of water, with local density (e.g., the height of the first peak) displaying no apparent correlation with macroscopic expectations (i.e., contact angle). An appropriately defined width of the interface (or depletion width) was found to be smaller than the size of a water molecule and showed only a weak correlation with the contact angle (44).

The layering of water at all interfaces and the lack of correlation between the local density and the interface hydrophobicity might appear surprising and counterintuitive at first, but significant theoretical and simulation work suggests that it is not. First, by deblurring the molecular structure at an oil-water liquid-liquid interface (71) or carefully defining an instantaneous vapor-liquid surface and measuring the density of water along its normal (72), layering becomes evident even though these interfaces are considered to be featureless. Layering at metal vapor-liquid interfaces is well known; it was first predicted theoretically (73) and then confirmed later by experiments (74). Also, for vapor-liquid interfaces of Lennard-Jones fluids at low temperatures, Katsov & Weeks (75) have shown that in the absence of capillary wave fluctuations, the intrinsic density profile (determined by excluded volume interactions) displays significant layering effects. In other words, layering of water at realistic hydrophobic surfaces is not surprising, but expected.

Second, and more importantly, solute-water attractions play fundamentally different roles in the hydration of small and large length-scale solutes (76–79). On the one hand, around small solutes, packing effects dominate (34, 80), and addition of dispersive attractions has relatively small effects on the vicinal density of water (78, 81). On the other hand, the interface of a large repulsive solute (or a wall) with water is significantly dewetted and vapor-liquid-like. At such an interface, perturbative ideas based on the classic Weeks-Chandler-Andersen (WCA) picture of liquids fail to capture the effects of solute-water attractions (80, 82). The reference vapor-liquid interface is soft and can be translated with little free-energetic cost. As a result, the local density of water is highly sensitive to attractions (or external fields) (76, 78). Even relatively weak attractions have been predicted to pull the interface closer (34), and the mean solvent density may no longer characterize the hydrophobicity of an interface, but the fluctuations in density might (34, 51). That is, although a realistic hydrophobic-water interface appears different from a vapor-water interface, significant similarities in the local water structure, and especially fluctuations, can still be expected.

Theoretical expectation of enhanced water density fluctuations near hydrophobic interfaces is borne out quantitatively by simulation data. **Figure 3*a,b*** shows the time dependency of water molecules in a large cuboid observation volume located near hydrophobic ($-CH_3$) and hydrophilic (-OH) interfaces, as obtained from equilibrium MD simulations. The average numbers of water molecules are similar and do not discriminate the two surfaces, as expected from **Figure 2**. However, larger fluctuations are apparent near the hydrophobic ($-CH_3$) surface. For small, methane-sized spherical observation volumes, the entire distribution, $p(N)$, of the number of water molecules in that volume can be measured using equilibrium MD simulations. **Figure 3*d*** shows that $p(N)$ distributions are wider (indicating enhanced fluctuations) near hydrophobic surfaces and gradually become narrower (indicating quenching of fluctuations) with increasing surface hydrophilicity.

Obtaining the entire $p(N)$ distribution in a large observation volume is not feasible in a typical MD simulation but can be achieved using the umbrella sampling method employed by Patel et al. (48). The full distributions more clearly highlight the enhancement of density fluctuations near hydrophobic solutes, which is reflected in the fat tails of $p(N)$ distributions, especially for large observation volumes (see **Figure 3*e***). The non-Gaussian nature of these low-N tails underscores the softness of hydrophobic-water interfaces, which are reminiscent of the vapor-liquid interface of water. Collectively, these recent studies point to local density fluctuations, and not the average density, as a robust measure of the hydrophobicity of the underlying surface.

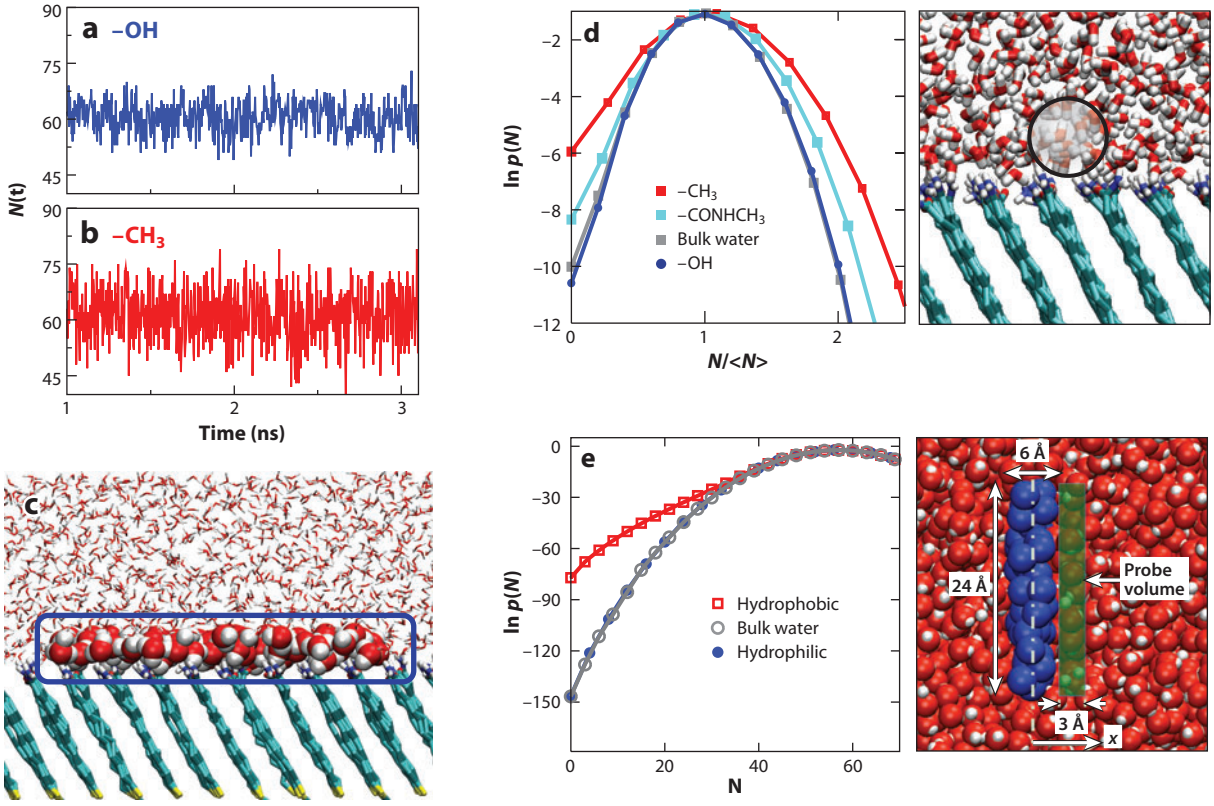

Figure 3

Fluctuations in water density characterize interface hydrophobicity. (*a*,*b*) Time series of the number of water molecules in a $2.5 \times 2.5 \times 0.3$ nm^3 cuboid observation volume (see panel *c*) at a hydrophilic (-OH) and a hydrophobic (-CH_3) surface, respectively. (*d*) Probability distributions for observing N heavy atoms, $p(N)$, in a small spherical observation volume ($r = 0.33$ nm) next to various self-assembled monolayer (SAM) surfaces and in the bulk solution (44). (*e*) $p(N)$ distributions in much larger $2.4 \times 2.4 \times 0.3$ nm^3 cuboid observation volumes next to hydrophobic and hydrophilic surfaces obtained using the umbrella sampling method of Patel et al. (48). In large observation volumes, $p(N)$ becomes significantly non-Gaussian with low-N fat tails near hydrophobic surfaces but near hydrophilic surfaces remains essentially identical to $p(N)$ in the bulk solution. (Panel *e* is courtesy of Amish Patel. Copyright © 2010 American Chemical Society.)

Compressibility of the Hydration Shell Water

Density fluctuations are intimately linked by statistical mechanics to both compressibility and pair correlations of water (83, 84). Enhancement of density fluctuations next to hydrophobic interfaces suggests enhancement of the local compressibility of water in the vicinity. Indeed, recent simulations of spherical hydrophobic solutes in water show that for nanoscopic solutes with radii of 1–2 nm, hydration shell compressibility—calculated either using density fluctuations or from the pressure response of the hydration shell density—can be several times that of bulk water. The addition of solute-water attractions quenches fluctuations and reduces the hydration shell compressibility (**Figure 4*a***) (85). The first hydration layer of various SAMs also displays similar characteristics (53) (**Figure 4*b***). The compressibility of the interfacial water layer next to the hydrophobic -CH_3 SAM is roughly three times that of bulk water, and the compressibility approaches the value for bulk water for -OH-terminated SAMs. Giovambattista et al. (49) and Bratko et al. (86) have

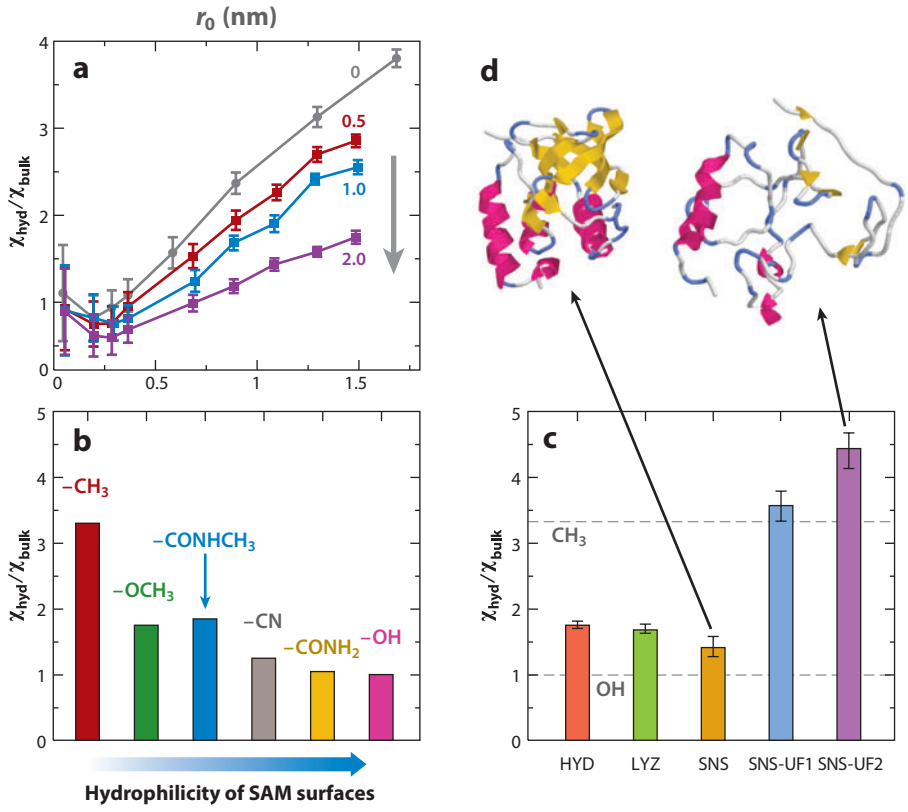

Figure 4

Compressibility, χ_{hyd}, of hydration shells of various solutes or interfaces obtained using the pressure derivative of local water density. (*a*) χ_{hyd} around simple, spherical nonpolar solutes from Sarupria et al. (85). As the solute size increases, χ_{hyd} increases, but is quenched by addition of solute-water attractions. The arrow indicates increasing solute-water attractions. (*b,c*) χ_{hyd} of various self-assembled monolayers and protein surfaces [hydrophobin (HYD), lysozyme (LYZ), staphnuclease (SNS)] from Acharya et al. (53). For SNS, χ_{hyd} around two unfolded (UF) conformations are also shown in panel (*c*). *(d)* A snapshot of the folded and one of the unfolded conformations of SNS. For ease of comparison, all data are normalized by the compressibility of pure water (4.5×10^{-5} bar^{-1}).

studied the compressibility of water confined between hydrophobic plates and have reported values higher than those for bulk water, highlighting the softness of the hydrophobic-water interface.

Hydration shell compressibility of proteins is of interest because it quantifies an important contribution to the response of the volumetric properties of proteins to hydrostatic pressure. Additionally, the connection between density fluctuations and hydrophobicity highlighted above may be used to characterize protein surfaces. At a broad level, one might ask, how hydrophobic/philic is the overall protein surface? Comparing the hydration shell compressibility of a few proteins with that of smooth, homogeneous SAM surfaces, Acharya et al. (53) find that, globally, the hydration shell of a folded globular protein is as compressible as that of a hydrophilic -OCH_3 SAM (**Figure 4*c***). When a protein unfolds, the hydration shell compressibility increases and becomes comparable with that at a hydrophobic -CH_3 SAM. This is consistent with the increased exposure of hydrophobic residues of proteins upon unfolding. Also, it provides additional insights into pressure denaturation of proteins, in which higher pressures stabilize (unfolded) states with

higher hydration shell compressibility and lower partial molar volume (87). Later in this review we show that what is hydrophobic on a protein's surface will depend on the local environment, i.e., the context matters, which will be important in mapping of protein surface hydrophobicity at a higher resolution.

Water Structure in the Hydration Shell

The structure of water in the hydration shell of hydrophobic solutes and at interfaces is expected to be intimately connected to hydrophobic hydration thermodynamics (88). Water structure is characterized by various inhomogeneous *n*-particle correlation functions, e.g., translational and orientational solute-water correlations characterize the one-particle density of water in the field of solute interactions. The quantities of interest here—density fluctuations, or alternatively, compressibility of a fluid in a given volume—are related to two-particle inhomogeneous fluid-fluid correlations (85). How are the enhanced compressibility or fluctuations at hydrophobic interfaces manifested in changes in water-water correlations?

For simplicity, we focus on water-water correlations in planes parallel to the interface. At a vapor-liquid interface (or near a hard wall), the in-plane water-water correlations display two key differences relative to bulk water-water correlations. First, the short-range correlations—which are governed by the competition between hydrogen bonding and excluded volume effects—are enhanced. Second, correlations are truly long range, spanning the length of the entire system and described by capillary wave fluctuations (**Figure 5*a*,*b***) (89–91). As attractions between the interface and water are dialed in, longer-range correlations are quenched (**Figure 5*d***), as is the case near a hydrophobic -CH_3 surface (not shown). However, the short-range behavior near a -CH_3 surface (**Figure 5*b***) or at other model hydrophobic surfaces (**Figure 5*d***) is remarkably similar to that at a water-vapor interface with a significantly enhanced first peak. These results suggest that although the local density of water is bulk-like or higher at hydrophobic interfaces, water-water correlations over nanoscale distances display characteristics that are quite similar to those at a vapor-water interface.

We argue, therefore, that experiments focusing on measurements of density fluctuations or water-water correlations could provide valuable information with regard to characterizing hydrophobic interfaces. Vaknin and coworkers (92) recently measured the structure factor of water at vapor-water interfaces. Doing similar measurements at solid-water interfaces would be challenging, especially given that most long-range correlations are quenched at realistic hydrophobic surfaces. To this end, perhaps, the use of superhydrophobic surfaces will provide a convenient starting point, as longer-range correlations are not expected to be quenched at such surfaces.

We briefly comment on water orientations as another aspect of water structure at interfaces. Orientational preferences of water molecules at hydrophobic interfaces were first reported in a seminal paper by Lee et al. in 1984 (93). Over the past decade, significant experimental work has focused on orientations and hydrogen bonding at vapor-water and hydrophobic interfaces using sum frequency generation (94–98), NMR, and various spectroscopic studies (99–101). Simulations show that in the 3–4-Å thick interfacial region, water dipoles lie predominantly parallel to the interface (4, 93, 102), whereas in the low-water-density tail, water molecules increasingly tend to give up one of their hydrogen bonds, as pointed out originally by Lee et al. (93). These dangling hydrogen bonds have been observed experimentally at vapor-water and oil-water interfaces. Recently, Ben Amotz and coworkers (99) have pointed to the similarity of orientational features for water near molecules as small as pentanol and near more extended surfaces. Thus, orientations of water may, in principle, uniquely characterize hydrophobic interfaces. However, strong orientational preferences are observed only in the thin (~3 Å) interfacial region, and at realistic

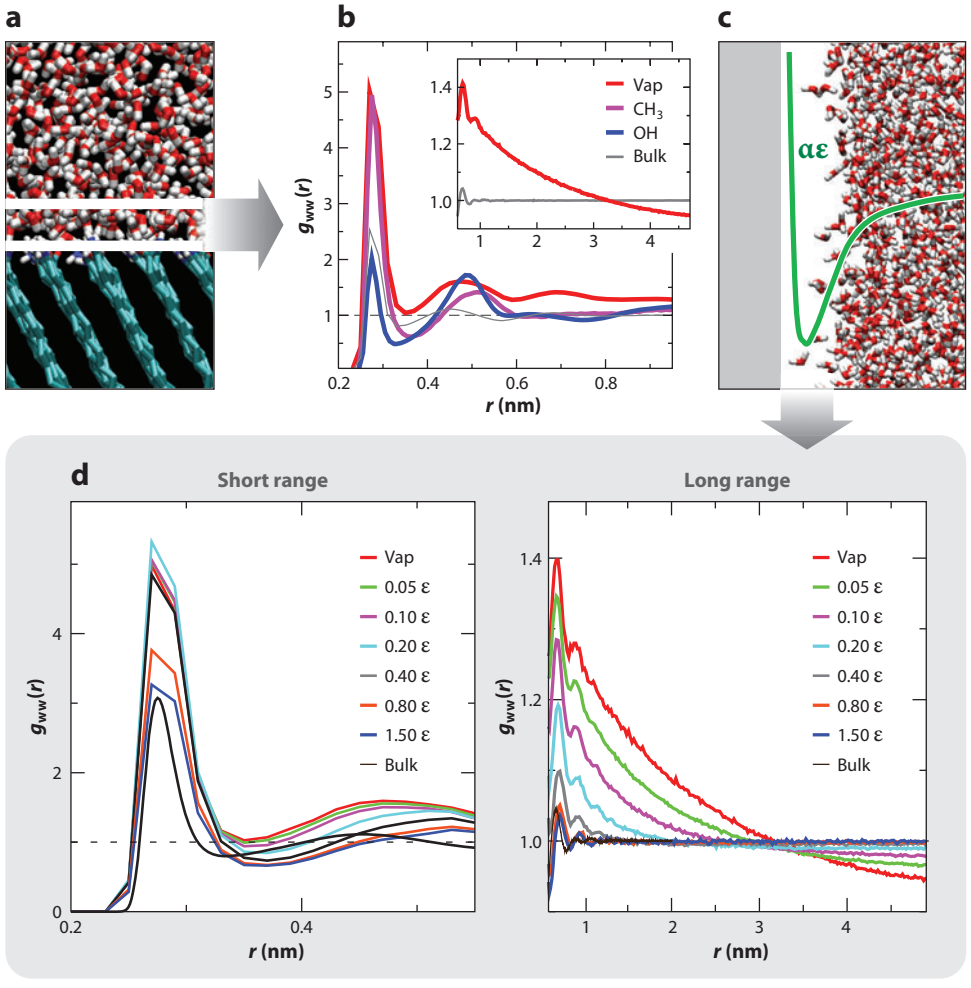

Figure 5

Water-water correlations in the interfacial plane. (*a*) Schematic showing the water slab at the interface in which transverse water-water pair correlations are measured. (*b*) Transverse correlations in bulk water, at a vapor-liquid water interface, and at -CH_3 and -OH surfaces (44). (*inset*) The long-range part of the water-water pair correlation function, $g_{ww}(r)$, at a vapor-water interface and in bulk water. (*c*) Schematic of a smooth wall interacting with a 9–3 potential with water. The strength of the wall-water interaction is characterized by the well depth, $\alpha\varepsilon$. (*d*) Short- and long-range pair correlations at such smooth 9–3 surfaces for various well depths, $\alpha\varepsilon$, where $\varepsilon = 1$ kJ mol^{-1}. Correlations for systems with seven different values of α, equal to 0 (vapor), 0.05, 0.10, 0.20, 0.40, 0.80, and 1.50, are shown. There are system-spanning correlations at vapor-water and superhydrophobic surfaces ($\alpha\varepsilon < 0.20$ kJ mol^{-1}). Addition of realistic attractions quenches long-range correlations, but short-range correlations are enhanced even at realistic hydrophobic surfaces ($\alpha\varepsilon < 0.60$ kJ mol^{-1}) (R. Godawat, S.N. Jamadagni, S. Garde, unpublished data).

hydrophilic surfaces, orientations will depend on the specific surface chemistry, especially on the presence of hydrogen bond donors and acceptors, which complicates the picture. On the other hand, simulations suggest that the effect of a hydrophobic interface on density fluctuations extends approximately a nanometer into the bulk phase (44, 48), which is longer ranged than the effects on orientations.

CONSEQUENCES OF FLUCTUATIONS FOR THE PHENOMENA AT INTERFACES

Solute Binding

One important and direct consequence of increased fluctuations at hydrophobic interfaces is that formation of a cavity (i.e., $N = 0$) is easier near the interface than in the bulk. Because the excess chemical potential of a hard sphere solute is related to the cavity formation probability via $\mu_{HS}^{ex} = -k_b T \ln[p(N = 0)]$, such solutes will bind favorably to hydrophobic surfaces and provide an alternative microscopic measure of interface hydrophobicity. Remarkably, the free energy of binding correlates almost linearly with macroscopic wettability (**Figure 6*a***). Such a correlation

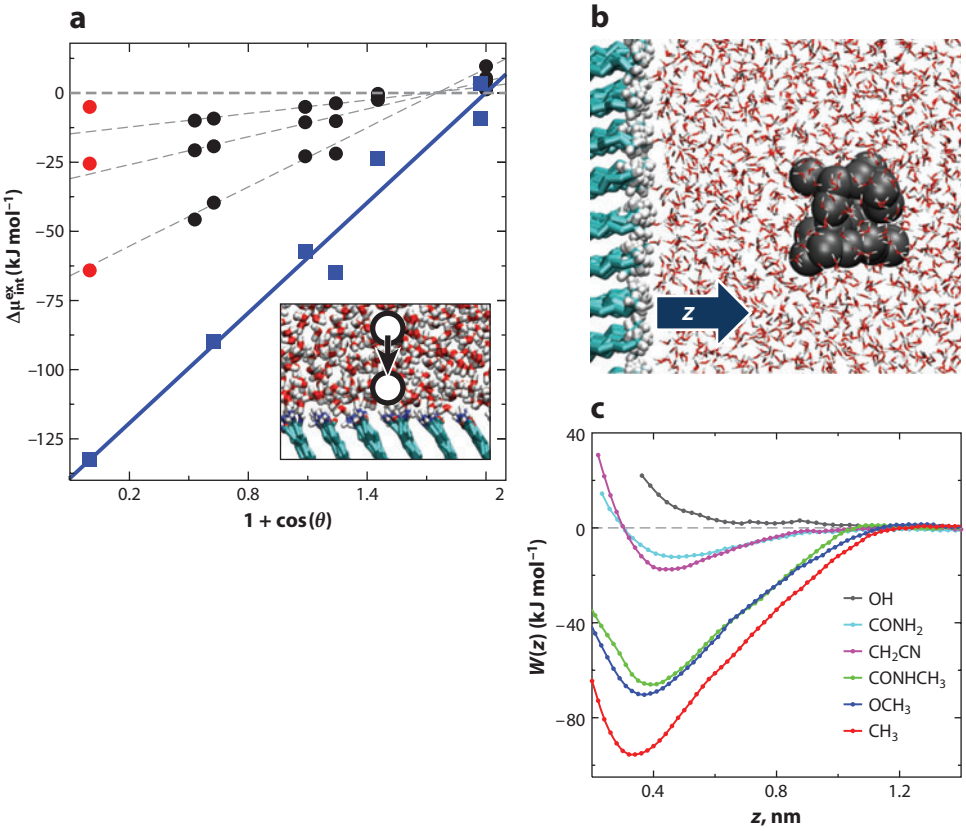

Figure 6

How interface hydrophobicity affects the binding of various solutes. (*a*) Excess chemical potential of purely repulsive Weeks-Chandler-Andersen solutes at various self-assembled monolayer (SAM)-water interfaces relative to their chemical potential in bulk water as a function of the macroscopic wettability of SAMs [data points indicated by black circles are from Godawat et al. (44)]. A linear correlation with surface wettability is seen, as the slope increases with solute size. The binding free energy of an attractive alkane-like hydrophobic 25-mer polymer is also shown [data points indicated by blue squares with a linear fit also in blue are from Jamadagni et al. (46)]. The red circles in (*a*) indicate values estimated at a water-vapor interface ($\cos\theta = -1$) (44, 46). (*b*,*c*) The simulation schematic and potentials of mean force (PMFs) for the binding of the polymer to various SAM surfaces. The minima in the PMFs in panel *c* correspond roughly to the location of the SAM-water interface.

is not restricted to hard sphere probe solutes. Hydration free energies of realistic hydrophobic solutes have contributions from cavity formation and from van der Waals interactions. The latter contribution depends mainly on the density of the surrounding medium, which does not change significantly at the interface of two condensed systems. As a result, the binding of a hydrophobic polymer, a more realistic solute, also displays a linear relation with macroscopic wettability (46). The polymer binds strongly to hydrophobic surfaces; as the surface becomes more polar and hydrophilic, the strength of binding reduces until water-mediated interactions repel the polymer from the most hydrophilic surface (**Figure 6*b*,*c***), which is qualitatively similar to experimental observations on proteins (56, 103). Schwartz and coworkers (104, 105) have recently pioneered the use of total internal reflection fluorescence microscopy to monitor the binding of individual surfactants or proteins to solid-liquid patterned surfaces or liquid-liquid interfaces. Although the resolution of patterns that can be detected is several micrometers, with advances in experimental technology, extension to the nanoscale regime may be possible. It would indeed be exciting if future experiments can test simulation results on the linear relationship between binding free energies and surface wettability.

Conformations of Flexible Molecules

Interfaces provide an inhomogeneous environment for flexible molecules and can significantly affect their conformational preferences. For example, hydrophobic polymers, which collapse into an ensemble of globular structures in water, when present at a hydrophobic surface adopt flat, quasi-2D pancake-like structures (45, 46). With increasing hydrophilicity of the interface, stable conformations gradually bead up, becoming globular near the most hydrophilic surfaces, similar to their behavior in bulk water.

Unfolding of proteins at the most hydrophobic vapor-liquid interface of water is well known (106, 107). Peptides or heteropolymers containing a sufficient number of hydrophobic groups will be pinned down to a flat hydrophobic surface (or to a vapor-water interface) and will adopt quasi-2D conformations. Recent work suggests that such interfaces (as well as those of nanoparticles) may nucleate β-sheet structures or aid fibril formation (108–115). Thus, bias toward flat structures, aided by intra- or intermolecular hydrogen bonding, may serve to stabilize β- or fibril-like structures. Given that cell interiors contain a large density of interfaces, more focused investigations of the role of hydrophobic interfaces in nucleating or promoting amyloid fibril formation are needed.

Dynamics

Both translational and rotational dynamics of water in the vicinity of hydrophobic solutes and interfaces have been investigated by experiments (116–119) and simulations (120–123). Experimental studies indicate a moderate slowdown in reorientational dynamics of water near hydrophobic solutes that has been confirmed by simulation studies (120). Qualitative connections between the slowdown of hydration dynamics and the negative entropy of hydration have been suggested (124). Near extended hydrophobic surfaces, enhanced fluctuations and a positive entropy of hydration suggest that water dynamics there could be faster than near hydrophilic surfaces. Simulations show that the translational diffusivity of water near a hydrophobic surface (e.g., a -CH_3 SAM) is comparable with that in bulk water but decreases significantly near hydrophilic (e.g., -OH SAM) surfaces (46, 125). In hydrophilic confinement, Castrillon et al. (121) observe a slowdown in both translational and rotational dynamics of water. They find that the effect of the interface on

rotational dynamics is limited to a region approximately 0.5 nm from the surface, whereas that on translational dynamics persists over a larger region (~1 nm).

Similar to water, we found that for hydrophobic polymers, the translational diffusivity is higher and conformational dynamics are faster at a hydrophobic interface relative to in the bulk water phase (45, 46). These observations of faster dynamics near extended flat hydrophobic surfaces imply that water as well as nonpolar solutes slide faster at hydrophobic interfaces, an observation consistent with fast water transport through carbon nanotube interiors, where significant hydrodynamic slip is observed (126–129).

Connections to Thermal Transport and Hydrodynamics

The hydrophobicity of an interface—whether characterized macroscopically by droplet contact angle or microscopically by density fluctuations, solute binding, or water correlations—represents one measure of coupling between water and a surface. Other measures of interfacial coupling also exist; for example, the thermal conductance of an interface [the inverse of the so-called Kapitza resistance (130)] is high when the two phases are strongly thermally coupled. Interfacial thermal conductance can be obtained using nonequilibrium MD simulations (70), which for -OH and -CH_3 SAM surfaces (in **Figure 2**) show quantitative agreement with experimental measurements (68). Furthermore, simulations of heat transfer at a range of SAM-water surfaces show that the interfacial thermal conductance varies linearly with the water droplet contact angle, indicating connections between interfacial thermal transport and wetting and hydrophobicity (70).

From a hydrodynamic perspective, the extent of stick (or slip) at an interface is another way to characterize interfacial coupling. Extensive simulations of water at diamond-like solid surfaces by the Netz group (125, 131) have shown that the magnitude of slip increases with increasing surface hydrophobicity. Collectively, these studies suggest qualitative connections between various methods of characterizing the extent of coupling between water and a solid surface. Developing theories to make these connections more quantitative will be an interesting and important direction to pursue (e.g., see Reference 125 and references therein for theoretical arguments connecting hydrodynamic slip to interfacial interactions and the contact angle). For thermal transport, developing a theory that takes into account interfacial solid-fluid interactions, in addition to bulk property mismatch, would constitute an important advance.

APPLICATIONS TO HETEROGENEOUS INTERFACES AND TO PROTEINS

Chemically Heterogeneous Flat Surfaces

How does the presence of a small number of hydrophilic groups affect the hydrophobicity of a background hydrophobic surface (and vice versa)? This is, perhaps, the first important question to consider regarding simple chemically heterogeneous surfaces. It can be addressed quantitatively using spatially resolved density fluctuation–based measures of hydrophobicity. Using a coarse-grained lattice gas description, Willard & Chandler (132) showed that isolated hydrophilic sites quench density fluctuations locally and pin the interface. Acharya et al. (53) considered effects of single head-group mutations in SAMs—one -OH group in a -CH_3 background and vice versa—on density fluctuations of water in the vicinity. They showed that density fluctuations not only identified the single mutations (**Figure 7**) but highlighted a striking asymmetry: A single -OH head group strongly quenched fluctuations in its vicinity in the -CH_3 background, whereas a single -CH_3 negligibly enhanced fluctuations in the -OH background. Extending these studies to larger hydrophobic

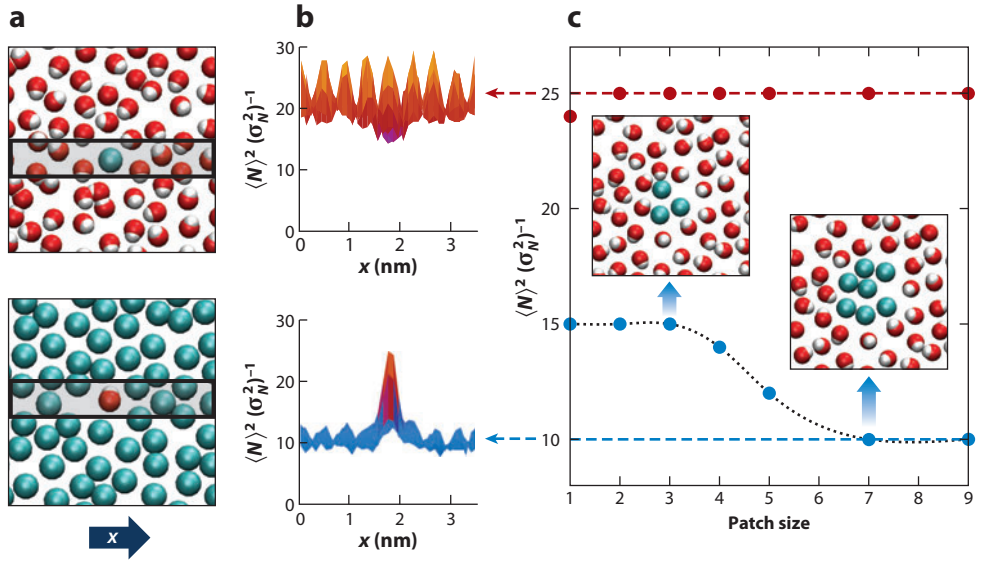

Figure 7

(*a*) Snapshot of surfaces with a hydrophobic (-CH_3) heterogeneity in a hydrophilic (-OH) background (*top*) and vice versa (*bottom*). (*b*) Spatially resolved (inverse) fluctuations in a methane-sized spherical observation volume of radius 0.33 nm next to the surfaces in panel *a* show the asymmetry in how hydrophilic and hydrophobic heterogeneities affect density fluctuations. The information theory formalism for the hydration of small solutes relates density fluctuations to the excess chemical potential of hard sphere solutes, $\mu_{HS}^{ex} \approx k_b T \langle N \rangle^2 / 2\sigma^2$ (39, 173). Thus, the vertical axis is roughly equal to twice the methane-sized hard sphere excess chemical potential at the interface in k_bT units. (*c*) Reciprocal of density fluctuations at the center of a contiguous patch containing $n = 1, 2, 3, 4, 5, 7, 9$ -CH_3 groups in an -OH background surface (*blue*) and vice versa (*red*). From Acharya et al. (53).

patches, Acharya et al. (53) showed that a contiguous domain of seven to nine -CH_3 groups (~1–1.5-nm diameter patch) is needed in the hydrophilic -OH background before its hydrophobicity (as measured by fluctuations) is comparable with that of a homogeneous -CH_3 surface (**Figure 7**).

This patch-size dependency in 2D space is qualitatively analogous to the length-scale dependency of hydrophobic hydration (33). The hydrophobicity of the CH_3 patch becomes independent of the patch size when it becomes large enough that water molecules can no longer maintain hydrogen bonds across the domain. Vicinal fluctuations then approach those seen at a homogeneous surface, resulting once again in a 1–2-nm crossover length scale. This 2D length-scale dependency manifests itself in the nonadditivity of surface tension (i.e., failure of linear models) for heterogeneous surfaces when the length scale of heterogeneity becomes subnanoscopic (133).

The hydration of chemically heterogeneous systems has received considerable attention in the context of confined systems using both coarse-grained (134) and atomistic simulations (50). "Water under confinement" has attracted enormous interest in the past decade (49, 50, 52, 135–138) because of its implications for a variety of important phenomena, including protein interactions, association, and aggregation; the specific role of water in cavities (139–142); and water phase behavior and transport through pores (126, 143, 144). Confinement can amplify the effects that would be observed at isolated surfaces. For example, the tendency to dewet an isolated hydrophobic surface is amplified, which leads to observation of capillary evaporation or a drying transition under hydrophobic confinements (50, 134). Also, adding a few hydrophilic groups to the surfaces can significantly reduce capillary drying (50, 134). How heterogeneous chemistry, patterning, and

topography affect the behavior of water under nanoscale confinements and its effects, in turn, on the association of surfaces will continue to be a rich problem for future studies.

Proteins

To map the hydrophobicity/hydrophilicity pattern of protein surfaces, hydropathy scales are frequently used (145, 146). These scales rank amino acids on the basis of their transfer free energies from nonpolar to aqueous phases. Trout and coworkers (147) have shown that an improved description is obtained by weighting the hydropathy scales with simulation-averaged solvent-exposed surface area. However, the problem that different scales do not necessarily agree in their ordering of amino acid hydrophobicity, or are quantitatively different when the ordering matches, remains. The results of Acharya et al. (53) and others (50, 132), however, point to the more difficult problem of context dependency (i.e., the importance of the local environment) in determining the effective hydrophobicity of a chemical moiety and highlight limitations inherent to context-independent descriptions.

Density fluctuation–based characterization naturally accounts for how water responds to local chemical and topographical context, as shown above. Siebert & Hummer (148) were the first to apply these ideas to proteins. They used molecular simulations—test particle insertions as well as probe-binding calculations—and inhomogeneous information theory to identify hydrophobic binding sites on different regions of a soluble analog of the *N*-peptide coiled coil of gp41 (IQN17). More recently, Acharya et al. (53) have used density fluctuation–based measures [e.g., binding of hydrophobic probes (see **Figure 8*a***)] to characterize the hydrophobicity map of the protein hydrophobin-II. They find that one face of the protein, which hydropathy scales predict to be rather hydrophobic, is weakly hydrophobic overall but contains a few strongly hydrophobic hot spots (**Figure 8*b***).

The practical success of density fluctuation–based measures for complex surfaces of proteins, e.g., to identify binding sites for a particular hydrophobic ligand, will depend on the ability to

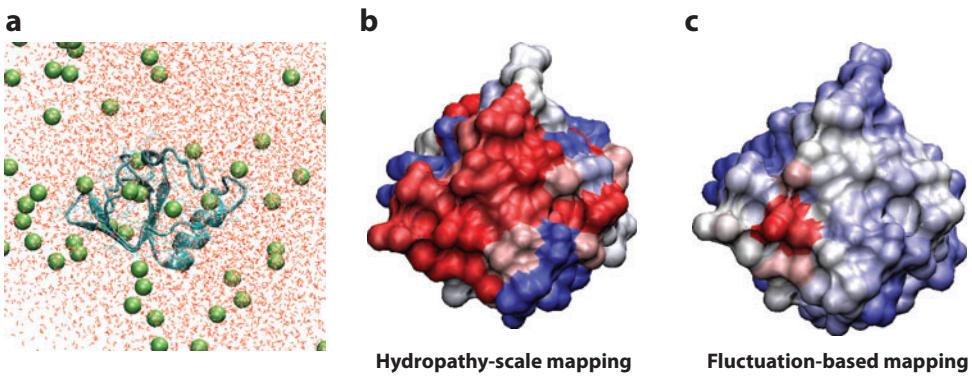

Figure 8

Mapping hydrophobicity of protein surfaces. (*a*) Schematic of a simulation of a protein in a solution containing small hydrophobic probe solutes (*green spheres*). By monitoring the concentration (or average density) of the probe solutes at different locations on the protein surface, one can identify hydrophobic patches. Other density fluctuation–based measures can also be implemented to obtain similar information. (*b*,*c*) Comparison of how a hydropathy-scale approach and the one outlined in panel *a*, respectively, map the hydrophobicity of the surface of hydrophobin-II. From Acharya et al. (53). Color scheme: red, hydrophobic; blue, hydrophilic.

quantify fluctuations in arbitrarily shaped observation volumes (of the shape of the ligand), to account for attractive interactions, and to account for protein fluctuations. Also, experimental verification of the predictions of density fluctuation–based characterization will be critical. In principle, probe-based interrogation of heterogeneous surfaces by simulations is not unlike that done experimentally in the multiple solvent crystal structures (MSCS) method, in which small chemical probes bind to proteins identified by X-ray crystallography (149), or chemical force spectroscopy, which uses a sensitive AFM tip with a chemical probe (150, 151). Studies along the lines of a recent report that combined NMR spectroscopy, MD simulations, and chromatography experiments (152) potentially provide powerful means to test density fluctuation–based hydrophobicity measures for specific protein systems of interest.

Rough Surfaces

Most surfaces of practical interest are chemically and topographically heterogeneous, and it is difficult to truly separate the effects of the two (153). Surface roughness has been long known to affect wetting properties of interfaces (154, 155); for example, the complex microstructure of a surface can lead to the lotus leaf effect, that is, the water repellency or superhydrophobicity and self-cleaning properties of leaves (156). It was hypothesized that micrometer-scale features in a hydrophobic surface will trap air (or vapor), thus creating a surface with a much higher effective surface hydrophobicity [called the Cassie state (157)]. However, adding roughness to already hydrophilic surfaces would further increase their hydrophilicity because water would wet the interstitial space as well [the so-called Wenzel state (158)]. In other words, roughness is expected to amplify the inherent character of the reference flat surface, be it hydrophobic or hydrophilic.

There has been significant effort to understand the effect of roughness on wetting using computer simulations (159–163). The emphasis has been on understanding how well the above ideas work when the roughness is in the nanoscale regime. To this end, for a Lennard-Jones fluid, Grzelak & Errington (160) recently presented an extensive study of the dependency of contact angles on surface roughness in the Wenzel regime. They showed that when the length scale of heterogeneity is larger than approximately 20 fluid diameters (or 10 nm), Wenzel predictions are near quantitative. Below that length scale, however, the Wenzel model overestimates the influence of roughness; i.e., the surface does not become as solvophilic as expected by the Wenzel equation when roughness is on the length scale of less than 10 nm (for argon fluid). We are not aware of a similarly systematic study in the Cassie-Baxter regime. Surface roughness on atomic length scales also did not seem to have significant influence on the wetting of different crystal faces by Lennard-Jones fluids (161).

For water, simulation studies indicate that surface roughness can have strong effects on wetting even at the nanoscale. Mittal & Hummer (162) show that for a 2D sinusoidal attractive surface, the solid-water interfacial tension changes from negative for a smooth surface to large positive for a rough surface with amplitude of ~3 Å and wavelength slightly larger than 1 nm. This sensitivity was attributed to the cost of deforming the hydrogen-bonded network of water to conform to the corrugations of the surface. Daub et al. (163) have also reported significant sensitivity of water droplet contact angle to nanoscale roughness for both hydrophobic and hydrophilic surfaces. Finally, in addition to static measures of wetting, roughness is expected to critically influence dynamics of fluids at interfaces, as reflected in contact angle hysteresis or contact line dynamics (164) or in metastability of droplets in Cassie or Wenzel states (159). As challenges in the fabrication of surfaces with well-defined features are overcome, a closer overlap in length and timescales in experiments and simulations will enable significantly deeper understanding of the connections between nanoscale surface topography and hydrophobicity.

CONCLUSIONS AND FUTURE DIRECTIONS

The central question we have focused on in this review has been that of identifying molecular signatures of hydrophobicity that correlate with macroscopic expectations. Such signatures are important for characterizing the hydrophobicity of complex macromolecules with chemical and topographical heterogeneities. The theory of hydration of idealized hydrophobic interfaces suggests high sensitivity of water density at the interface to attractive interactions, which cannot be described by standard perturbative treatments. Correspondingly, simulations show that the vicinal density of water correlates poorly with hydrophobicity (44). Theoretical developments suggested that water density fluctuations could serve as a potential informative measure of hydrophobicity (34, 51), and this expectation has now been borne out by several molecular simulation studies (44, 48, 85). Density fluctuations are enhanced at hydrophobic interfaces and gradually suppressed with increasing surface hydrophilicity. Cavity formation free energies or, alternatively, the free energy of binding of hydrophobic solutes to an interface, quantities that are determined by density fluctuations, display a monotonic (frequently linear) relationship with the macroscopic contact angle (44). Enhanced fluctuations at hydrophobic interfaces are also reflected in related statistical mechanical measures, namely local compressibility and water pair correlation functions. The compressibility of hydration shells of simple spherical solutes (85) and of atomically detailed SAM surfaces is several times higher than that of bulk water and decreases with increasing solute-water attractions or surface polarity (53). Spatial resolution of density fluctuations can identify isolated chemical heterogeneities (47, 53) and, importantly, highlights the context dependency of the hydrophobicity of a chemical moiety. In the remainder of this section, we highlight promising avenues for further research that build on the work reviewed so far.

Hydration Data Bank

The establishment of the Protein Data Bank (PDB) as a repository for crystallographic and NMR-derived structures of proteins that is accessible to researchers all over the world has been pivotal in today's structural biology revolution. These structures, however, contain little or no information about hydration water, which plays a key role in interactions of proteins in solution. Following the work reviewed here on mapping chemically heterogeneous surfaces, we think that creation of a similar Hydration Data Bank will have a transformative effect on biology and biochemistry. Such a data bank can serve as a repository for information critical to characterizing the behavior of hydration water—density fluctuations, structure, and dynamics—around proteins. With modern computing resources and novel parallel processing paradigms (165), molecular simulations of thousands of proteins could be performed and information about hydration water collected to generate hydration maps. Such a database will be of tremendous value to researchers investigating a variety of phenomena in which hydrophobic interactions play an important role, including protein hydration (166), protein-protein interactions (167–171), bioseparation processes (152), and drug discovery and design (172).

Confinement and Assembly

The inherent tendency to dewet a hydrophobic surface is amplified by confined environments. Behavior of water under confinement is also relevant when two proteins or biological surfaces come together. Understanding how the hydrophobicity of patches is affected by the geometric/confinement context and how that affects water-mediated interactions will not only be relevant

to protein interactions but also may assist the design of particles with patches for recognition and directed assembly.

Effect of Cosolvents and Additives

Cosolvents and additives are known to affect the solubility as well as interactions of hydrophobic solutes in water (21–24). For example, typical salts suppress density fluctuations in their vicinity, thereby expelling hydrophobic solutes from that region (173). Denaturants such as guanidinium chloride and urea also affect hydrophobic interactions via direct interactions (27, 30). Clearly, interfacial enhancement or depletion of additives will affect the behavior of water and especially the density fluctuations in the interfacial region. This raises the interesting possibility that the effective hydrophobicity of an interface, especially of patches on a heterogeneous one, can be manipulated using solution additives. This is a promising direction for further research.

Dynamics at Interfaces

Simulations show that water diffusivity is higher at extended hydrophobic surfaces and is suppressed near hydrophilic ones (46). Translational and conformational dynamics of flexible hydrophobic molecules also show similar trends (45, 46). Experimentally measuring conformational dynamics of molecules such as peptides or polymers at interfaces using various fluorescence or spectroscopic tools (174) could serve as a relatively direct probe of the dynamics and fluctuations in interfacial environments. Also, density fluctuations leading instantaneously to formation of a cavity or a high-density region is a many-body phenomenon. Whether these phenomena can be driven externally by coupling to periodic pumping of energy (e.g., via driven oscillations of a flexible interface), thereby amplifying and/or accelerating cavity formation, is not known (175) and represents a rich direction to explore.

Coarse-Grained Simulations

To access large length scales and long timescales relevant to macromolecular assembly, interest is growing in developing coarse-grained models for water and molecular systems (176–178) such as those that represent water molecules using short-range and spherically symmetric potentials, or even replace 3–4 water molecules with a single "bead" (177). Such models have been useful in studies of the self-assembly of lipid bilayer systems or structural phase transitions in surfactant systems (179, 180). The work reviewed here shows that capturing the nature of density fluctuations and associated quantities will be important for hydrophobically driven assembly.

To this end, approaches at both ends of the spectrum, from highly coarse-grained methods—e.g., applications of generalized mean field theory (181), LCW theory (33), and related efficient numerical implementations (40)—to those containing more detailed (but computationally efficient) models of water, will play a role. For the latter, a water model that preserves the atomic description, associated hydrogen bonding and excluded volume, and a correct description of density fluctuations, but at the same time eliminates the need for calculating long-range electrostatics, would be desirable. A Gaussian truncated water with associated corrections from local molecular field theories represents a promising candidate (182, 183). Further validation of such water models for a variety of interfacial systems, as well as efforts to incorporate them into MD engines such as GROMACS (184, 185) or NAMD (186), will enable their use for studying much larger systems than currently possible.

DISCLOSURE STATEMENT

The authors are not aware of any affiliations, memberships, funding, or financial holdings that might be perceived as affecting the objectivity of this review.

ACKNOWLEDGMENTS

We acknowledge numerous insightful discussions with David Chandler, John D. Weeks, Gerhard Hummer, Lawrence R. Pratt, Henry S. Ashbaugh, Amish Patel, Sapna Sarupria, Gaurav Goel, Thomas Truskett, and Pablo G. Debenedetti. We thank Hari Acharya and Srivathsan Vembanur for making results of their work available to us. S.G. gratefully acknowledges partial financial support from NSF, Nanoscale Science and Engineering Research Center Grant DMR-0642573; a New York State NYSTAR program grant to the Rensselaer Nanotechnology Center; and NSF-BES 0933169 and CBET 0967937 grants. We acknowledge the computing support of the Computational Center for Nanotechnology Innovations at Rensselaer.

LITERATURE CITED

1. Kauzmann W. 1959. Some factors in the interpretation of protein denaturation. *Adv. Protein Chem.* 14:1–63
2. Tanford C. 1962. Contribution of hydrophobic interactions to stability of globular conformation of proteins. *J. Am. Chem. Soc.* 84:4240–47
3. Dill KA. 1990. Dominant forces in protein folding. *Biochemistry* 29:7133–55
4. Pratt LR. 2002. Molecular theory of hydrophobic effects: "She is too mean to have her name repeated." *Annu. Rev. Phys. Chem.* 53:409–36
5. Tanford C. 1997. How protein chemists learned about the hydrophobic factor. *Protein Sci.* 6:1358–66
6. Pratt LR, Chandler D. 1977. Theory of hydrophobic effect. *J. Chem. Phys.* 67:3683–704
7. Pangali C, Rao M, Berne BJ. 1979. Hydrophobic hydration around a pair of apolar species in water. *J. Chem. Phys.* 71:2982–90
8. Pratt LR, Chandler D. 1980. Effects of solute-solvent attractive forces on hydrophobic correlations. *J. Chem. Phys.* 73:3434–41
9. Smith DE, Zhang L, Haymet ADJ. 1992. Entropy of association of methanes in water: a new molecular dynamics computer simulation. *J. Am. Chem. Soc.* 114:5875–76
10. Guillot B, Guissani Y. 1993. A computer-simulation study of the temperature-dependence of the hydrophobic hydration. *J. Chem. Phys.* 99:8075–94
11. Lazaradis T, Paulaitis ME. 1992. Entropy of hydrophobic hydration: A new statistical mechanical formulation. *J. Phys. Chem.* 96:3847–55
12. Ludemann S, Schreiber H, Abseher R, Steinhauser O. 1996. The influence of temperature on pairwise hydrophobic interactions of methane-like particles: a molecular dynamics study of free energy. *J. Chem. Phys.* 104:286–95
13. Silverstein KAT, Haymet ADJ, Dill KA. 1998. A simple model of water and the hydrophobic effect. *J. Am. Chem. Soc.* 120:3166–75
14. Garde S, Garcia AE, Pratt LR, Hummer G. 1999. Temperature dependence of the solubility of nonpolar gases in water. *Biophys. Chem.* 78:21–32
15. Garde S, Hummer G, Garcia AE, Paulaitis ME, Pratt LR. 1996. Origin of entropy convergence in hydrophobic hydration and protein folding. *Phys. Rev. Lett.* 77:4966–68
16. Huang DM, Chandler D. 2000. Temperature and length scale dependence of hydrophobic effects and their possible implications for protein folding. *Proc. Natl. Acad. Sci. USA* 97:8324–27
17. Wallqvist A. 1992. Pressure dependence of methane solvation in aqueous mixtures and the relation to the structure of liquid water. *J. Chem. Phys.* 96:1655–56

18. Hummer G, Garde S, Garcia AE, Paulaitis ME, Pratt LR. 1998. The pressure dependence of hydrophobic interactions is consistent with the observed pressure denaturation of proteins. *Proc. Natl. Acad. Sci. USA* 95:1552–55
19. Ghosh T, Garcia AE, Garde S. 2001. Molecular dynamics simulations of pressure effects on hydrophobic interactions. *J. Am. Chem. Soc.* 123:10997–1003
20. Smith PE. 1999. Computer simulation of cosolvent effects on hydrophobic hydration. *J. Phys. Chem. B* 103:525–34
21. Kalra A, Tugcu N, Cramer SM, Garde S. 2001. Salting-in and salting-out of hydrophobic solutes in aqueous salt solutions. *J. Phys. Chem. B* 105:6380–86
22. Ghosh T, Kalra A, Garde S. 2005. On the salt-induced stabilization of pair and many-body hydrophobic interactions. *J. Phys. Chem. B* 109:642–51
23. Thomas AS, Elcock AH. 2007. Molecular dynamics simulations of hydrophobic associations in aqueous salt solutions indicate a connection between water hydrogen bonding and the Hofmeister effect. *J. Am. Chem. Soc.* 129:14887–98
24. Athawale MV, Dordick JS, Garde SG. 2005. Osmolyte trimethylamine-*n*-oxide does not affect the strength of hydrophobic interactions: origin of osmolyte compatibility. *Biophys. J.* 89:858–66
25. Zhang YJ, Cremer PS. 2010. Chemistry of Hofmeister anions and osmolytes. *Annu. Rev. Phys. Chem.* 61:63–83
26. Hua L, Zhou R, Thirumalai D, Berne BJ. 2008. Urea denaturation by stronger dispersion interactions with proteins than water implies a 2-stage unfolding. *Proc. Natl. Acad. Sci. USA* 105:16928–33
27. Godawat R, Jamadagni SN, Garde S. 2010. Unfolding of hydrophobic polymers in guanidinium chloride solutions. *J. Phys. Chem. B* 114:2246–54
28. O'Brien EP, Dima RI, Brooks B, Thirumalai D. 2007. Interactions between hydrophobic and ionic solutes in aqueous guanidinium chloride and urea solutions: lessons for protein denaturation mechanism. *J. Am. Chem. Soc.* 129:7346–53
29. England JL, Pande VS, Haran G. 2008. Chemical denaturants inhibit the onset of dewetting. *J. Am. Chem. Soc.* 130:11854–55
30. Zangi R, Zhou RH, Berne BJ. 2009. Urea's action on hydrophobic interactions. *J. Am. Chem. Soc.* 105:16928–33
31. Baynes BM, Trout BL. 2003. Proteins in mixed solvents: A molecular-level perspective. *J. Phys. Chem. B* 107:14058–67
32. Stillinger FH. 1973. Structure in aqueous solutions of nonpolar solutes from the standpoint of scaled-particle theory. *J. Solut. Chem.* 2:141–58
33. Lum K, Chandler D, Weeks JD. 1999. Hydrophobicity at small and large length scales. *J. Phys. Chem. B* 103:4570–77
34. Chandler D. 2005. Interfaces and the driving force of hydrophobic assembly. *Nature* 437:640–47
35. Huang DM, Geissler PL, Chandler D. 2001. Scaling of hydrophobic solvation free energies. *J. Phys. Chem. B* 105:6704–9
36. Katsov K, Weeks JD. 2001. On the mean field treatment of attractive interactions in nonuniform simple fluids. *J. Phys. Chem. B* 105:6738–44
37. Huang DM, Chandler D. 2000. Cavity formation and the drying transition in the Lennard-Jones fluid. *Phys. Rev. E* 61:1501–6
38. Ashbaugh HS, Pratt LR. 2006. Colloquium: scaled particle theory and the length scales of hydrophobicity. *Rev. Mod. Phys.* 78:159–78
39. Hummer G, Garde S, Garcia AE, Pohorille A, Pratt LR. 1996. An information theory model of hydrophobic interactions. *Proc. Natl. Acad. Sci. USA* 93:8951–55
40. ten Wolde PR, Chandler D. 2002. Drying-induced hydrophobic polymer collapse. *Proc. Natl. Acad. Sci. USA* 99:6539–43
41. Rajamani S, Truskett TM, Garde S. 2005. Hydrophobic hydration from small to large lengthscales: Understanding and manipulating the crossover. *Proc. Natl. Acad. Sci. USA* 102:9475–80
42. Hummer G, Garde S. 1998. Cavity expulsion and weak dewetting of hydrophobic solutes in water. *Phys. Rev. Lett.* 80:4193–96

43. Egelstaf PA, Widom B. 1970. Liquid surface tension near triple point. *J. Chem. Phys.* 53:2667–69
44. Godawat R, Jamadagni SN, Garde S. 2009. Characterizing hydrophobicity of interfaces by using cavity formation, solute binding, and water correlations. *Proc. Natl. Acad. Sci. USA* 106:15119–24
45. Jamadagni SN, Godawat R, Dordick JS, Garde S. 2009. How interfaces affect hydrophobically driven polymer folding. *J. Phys. Chem. B* 113:4093–101
46. Jamadagni SN, Godawat R, Garde S. 2009. How surface wettability affects the binding, folding, and dynamics of hydrophobic polymers at interfaces. *Langmuir* 25:13092–99
47. Willard AP, Chandler D. 2008. The role of solvent fluctuations in hydrophobic assembly. *J. Phys. Chem. B* 112:6187–92
48. Patel AJ, Varilly P, Chandler D. 2010. Fluctuations of water near extended hydrophobic and hydrophilic surfaces. *J. Phys. Chem. B* 114:1632–37
49. Giovambattista N, Rossky PJ, Debenedetti PG. 2006. Effect of pressure on the phase behavior and structure of water confined between nanoscale hydrophobic and hydrophilic plates. *Phys. Rev. E* 73:041604
50. Giovambattista N, Debenedetti PG, Rossky PJ. 2007. Hydration behavior under confinement by nanoscale surfaces with patterned hydrophobicity and hydrophilicity. *J. Phys. Chem. C* 111:1323–32
51. Berne BJ, Weeks JD, Zhou RH. 2009. Dewetting and hydrophobic interaction in physical and biological systems. *Annu. Rev. Phys. Chem.* 60:85–103
52. Rasaiah JC, Garde S, Hummer G. 2008. Water in nonpolar confinement: from nanotubes to proteins and beyond. *Annu. Rev. Phys. Chem.* 59:713–40
53. Acharya H, Vembanur S, Jamadagni SN, Garde S. 2010. Mapping hydrophobicity at the nanoscale: applications to heterogeneous surfaces and proteins. *Faraday Discuss.* 146:353–65
54. Ball P. 2008. Water as an active constituent in cell biology. *Chem. Rev.* 108:74–108
55. Israelachvili JN. 1992. *Intermolecular and Surface Forces*. New York: Academic. 2nd ed.
56. Sigal GB, Mrksich M, Whitesides GM. 1998. Effect of surface wettability on the adsorption of proteins and detergents. *J. Am. Chem. Soc.* 120:3464–73
57. Granick S, Bae SC. 2008. Chemistry: a curious antipathy for water. *Science* 322:1477–78
58. Mezger M, Reichert H, Schoder S, Okasinski J, Schroder H, et al. 2006. High-resolution in situ X-ray study of the hydrophobic gap at the water-octadecyl-trichlorosilane interface. *Proc. Natl. Acad. Sci. USA* 103:18401–4
59. Jensen TR, Jensen MØ, Reitzel N, Balashev K, Peters GH, et al. 2003. Water in contact with extended hydrophobic surfaces: Direct evidence of weak dewetting. *Phys. Rev. Lett.* 90:086101
60. Kashimoto K, Yoon J, Hou BY, Chen CH, Lin BH, et al. 2008. Structure and depletion at fluorocarbon and hydrocarbon/water liquid/liquid interfaces. *Phys. Rev. Lett.* 101:086101
61. Ocko BM, Dhinojwala A, Daillant J. 2008. Comment on "How water meets a hydrophobic surface." *Phys. Rev. Lett.* 101:039601
62. Poynor A, Hong L, Robinson IK, Granick S, Fenter PA, Zhang Z. 2008. Reply to comment on "How water meets a hydrophobic surface." *Phys. Rev. Lett.* 101:039602
63. Seo YS, Satija S. 2006. No intrinsic depletion layer on a polystyrene thin film at a water interface. *Langmuir* 22:7113–16
64. Schwendel D, Hayashi T, Dahint R, Pertsin A, Grunze M, et al. 2003. Interaction of water with self-assembled monolayers: neutron reflectivity measurements of the water density in the interface region. *Langmuir* 19:2284–93
65. Steitz R, Gutberlet T, Hauss T, Klosgen B, Krastev R, et al. 2003. Nanobubbles and their precursor layer at the interface of water against a hydrophobic substrate. *Langmuir* 19:2409–18
66. Maccarini M, Steitz R, Himmelhaus M, Fick J, Tatur S, et al. 2007. Density depletion at solid-liquid interfaces: a neutron reflectivity study. *Langmuir* 23:598–608
67. Takata Y, Cho JHJ, Law BM, Aratono M. 2006. Ellipsometric search for vapor layers at liquid-hydrophobic solid surfaces. *Langmuir* 22:1715–21
68. Ge ZB, Cahill DG, Braun PV. 2006. Thermal conductance of hydrophilic and hydrophobic interfaces. *Phys. Rev. Lett.* 96:186101
69. Chattopadhyay S, Uysal A, Stripe B, Ha YG, Marks TJ, et al. 2010. How water meets a very hydrophobic surface. *Phys. Rev. Lett.* 105:037803

70. Shenogina N, Godawat R, Keblinski P, Garde S. 2009. How wetting and adhesion affect thermal conductance of a range of hydrophobic to hydrophilic aqueous interfaces. *Phys. Rev. Lett.* 102:156101
71. Ashbaugh HS, Pratt LR, Paulaitis ME, Clohecy J, Beck TL. 2005. Deblurred observation of the molecular structure of an oil-water interface. *J. Am. Chem. Soc.* 127:2808–9
72. Willard AP, Chandler D. 2010. Instantaneous liquid interfaces. *J. Phys. Chem. B* 114:1954–58
73. Develyn MP, Rice SA. 1981. Structure in the density profile at the liquid-metal-vapor interface. *Phys. Rev. Lett.* 47:1844–47
74. Magnussen OM, Ocko BM, Regan MJ, Penanen K, Pershan PS, Deutsch M. 1995. X-ray reflectivity measurements of surface layering in liquid mercury. *Phys. Rev. Lett.* 74:4444–47
75. Katsov K, Weeks JD. 2002. Incorporating molecular scale structure into the van der Waals theory of the liquid-vapor interface. *J. Phys. Chem. B* 106:8429–36
76. Huang DM, Chandler D. 2002. The hydrophobic effect and the influence of solute-solvent attractions. *J. Phys. Chem. B* 106:2047–53
77. Goel G, Athawale MV, Garde S, Truskett TM. 2008. Attractions, water structure, and thermodynamics of hydrophobic polymer collapse. *J. Phys. Chem. B* 112:13193–96
78. Athawale MV, Jamadagni SN, Garde S. 2009. How hydrophobic hydration responds to solute size and attractions: Theory and simulations. *J. Chem. Phys.* 131:115102
79. Ashbaugh HS, Paulaitis ME. 2001. Effect of solute size and attractive interactions on hydration water structure around hydrophobic solutes. *J. Am. Chem. Soc.* 123:10721–28
80. Weeks JD, Chandler D, Andersen HC. 1971. Role of repulsive forces in determining equilibrium structure of simple liquids. *J. Chem. Phys.* 54:5237–47
81. Chandler D, Andersen HC. 1972. Optimized cluster expansions for classical fluids. 2. Theory of molecular liquids. *J. Chem. Phys.* 57:1930–37
82. Weeks JD. 2002. Connecting local structure to interface formation: a molecular scale van der Waals theory of nonuniform liquids. *Annu. Rev. Phys. Chem.* 53:533–62
83. McQuarrie DA. 2000. *Statistical Mechanics*. Sausalito, CA: Univ. Sci. Books
84. Hansen JP, McDonald IR. 2006. *Theory of Simple Liquids.* New York: Academic. 3rd ed.
85. Sarupria S, Garde S. 2009. Quantifying water density fluctuations and compressibility of hydration shells of hydrophobic solutes and proteins. *Phys. Rev. Lett.* 103:037803
86. Bratko D, Curtis RA, Blanch HW, Prausnitz JM. 2001. Interaction between hydrophobic surfaces with metastable intervening liquid. *J. Chem. Phys.* 115:3873–77
87. Sarupria S, Ghosh T, Garcia AE, Garde S. 2010. Studying pressure denaturation of a protein by molecular dynamics simulations. *Proteins* 78:1641–51
88. Ben-Naim A. 1980. *Hydrophobic Interactions*. New York: Plenum
89. Weeks JD. 1977. Structure and thermodynamics of liquid-vapor interface. *J. Chem. Phys.* 67:3106–21
90. Kalos MH, Percus JK, Rao M. 1977. Structure of a liquid-vapor interface. *J. Stat. Phys.* 17:111–36
91. Evans R. 1979. Nature of the liquid-vapour interface and other topics in the statistical mechanics of nonuniform, classical fluids. *Adv. Phys.* 28:143–200
92. Vaknin D, Bu W, Travesset A. 2008. Extracting the pair distribution function of liquids and liquid-vapor surfaces by grazing incidence X-ray diffraction mode. *J. Chem. Phys.* 129:044504
93. Lee CY, McCammon JA, Rossky PJ. 1984. The structure of liquid water at an extended hydrophobic surface. *J. Chem. Phys.* 80:4448–55
94. Walker DS, Richmond GL. 2007. Understanding the effects of hydrogen bonding at the vapor-water interface: vibrational sum frequency spectroscopy of H_2O/HOD/D_2O mixtures studied using molecular dynamics simulations. *J. Phys. Chem. C* 111:8321–30
95. Buch V, Tarbuck T, Richmond GL, Groenzin H, Li I, Shultz MJ. 2007. Sum frequency generation surface spectra of ice, water, and acid solution investigated by an exciton model. *J. Chem. Phys.* 127:204710
96. Ji N, Ostroverkhov V, Tian CS, Shen YR. 2008. Characterization of vibrational resonances of water-vapor interfaces by phase-sensitive sum-frequency spectroscopy. *Phys. Rev. Lett.* 100:096102
97. Tian CS, Shen YR. 2009. Structure and charging of hydrophobic material/water interfaces studied by phase-sensitive sum-frequency vibrational spectroscopy. *Proc. Natl. Acad. Sci. USA* 106:15148–53
98. Tian CS, Shen YR. 2009. Sum-frequency vibrational spectroscopic studies of water/vapor interfaces. *Chem. Phys. Lett.* 470:1–6

99. Perera PN, Fega KR, Lawrence C, Sundstrom EJ, Tomlinson-Phillips J, Ben-Amotz D. 2009. Observation of water dangling OH bonds around dissolved nonpolar groups. *Proc. Natl. Acad. Sci. USA* 106:12230–34
100. Sovago M, Campen RK, Wurpel GWH, Muller M, Bakker HJ, Bonn M. 2008. Vibrational response of hydrogen-bonded interfacial water is dominated by intramolecular coupling. *Phys. Rev. Lett.* 100:173901
101. Stirnemann G, Rossky PJ, Hynes JT, Laage D. 2010. Water reorientation, hydrogen bond dynamics, and 2D-IR spectroscopy next to an extended hydrophobic surface. *Faraday Discuss.* 146:263–81
102. Choudhury N, Pettitt BM. 2005. On the mechanism of hydrophobic association of nanoscopic solutes. *J. Am. Chem. Soc.* 127:3556–67
103. Sethuraman A, Han M, Kane RS, Belfort G. 2004. Effect of surface wettability on the adhesion of proteins. *Langmuir* 20:7779–88
104. Honciuc A, Baptiste DJ, Schwartz DK. 2009. Hydrophobic interaction microscopy: mapping the solid/liquid interface using amphiphilic probe molecules. *Langmuir* 25:4339–42
105. Walder R, Schwartz DK. 2010. Single molecule observations of multiple protein populations at the oil-water interface. *Langmuir* 26:13364–67
106. Yano YF. 2007. Interesting features of liquid-vapor interfaces observed by X-ray reflection: protein unfolding at interfaces. *Am. Inst. Phys. Conf. Proc.* 902:93–95
107. Lu JR, Perumal S, Zhao XB, Miano F, Enea V, et al. 2005. Surface-induced unfolding of human lactoferrin. *Langmuir* 21:3354–61
108. Jean L, Lee CF, Lee C, Shaw M, Vaux DJ. 2010. Competing discrete interfacial effects are critical for amyloidogenesis. *FASEB J.* 24:309–17
109. Mukherjee S, Chowdhury P, Gai F. 2009. Effect of dehydration on the aggregation kinetics of two amyloid peptides. *J. Phys. Chem. B* 113:531–35
110. Stefani M. 2008. Protein folding and misfolding on surfaces. *Int. J. Mol. Sci.* 9:2515–42
111. Lee JH, Bhak G, Lee SG, Paik SR. 2008. Instantaneous amyloid fibril formation of α-synuclein from the oligomeric granular structures in the presence of hexane. *Biophys. J.* 95:L16–18
112. Linse S, Cabaleiro-Lago C, Xue WF, Lynch I, Lindman S, et al. 2007. Nucleation of protein fibrillation by nanoparticles. *Proc. Natl. Acad. Sci. USA* 104:8691–96
113. Cavalli S, Handgraaf JW, Tellers EE, Popescu DC, Overhand M, et al. 2006. Two-dimensional ordered β-sheet lipopeptide monolayers. *J. Am. Chem. Soc.* 128:13959–66
114. Nichols MR, Moss MA, Reed DK, Hoh JH, Rosenberry TL. 2005. Rapid assembly of amyloid-β peptide at a liquid/liquid interface produces unstable β-sheet fibers. *Biochemistry* 44:165–73
115. Schladitz C, Vieira EP, Hermel H, Mohwald H. 1999. Amyloid-β-sheet formation at the air-water interface. *Biophys. J.* 77:3305–10
116. Bakulin AA, Liang C, Jansen TL, Wiersma DA, Bakker HJ, Pshenichnikov MS. 2009. Hydrophobic solvation: A 2D IR spectroscopic inquest. *Acc. Chem. Res.* 42:1229–38
117. Wachter W, Buchner R, Hefter G. 2006. Hydration of tetraphenylphosphonium and tetraphenylborate ions by dielectric relaxation spectroscopy. *J. Phys. Chem. B* 110:5147–54
118. Shimizu A, Fumino K, Yukiyasu K, Taniguchi Y. 2000. NMR studies on dynamic behavior of water molecule in aqueous denaturant solutions at 25°C: effects of guanidine hydrochloride, urea and alkylated ureas. *J. Mol. Liq.* 85:269–78
119. Qvist J, Halle B. 2008. Thermal signature of hydrophobic hydration dynamics. *J. Am. Chem. Soc.* 130:10345–53
120. Laage D, Stirnemann G, Hynes JT. 2009. Why water reorientation slows without iceberg formation around hydrophobic solutes. *J. Phys. Chem. B* 113:2428–35
121. Castrillon SRV, Giovambattista N, Aksay IA, Debenedetti PG. 2009. Evolution from surface-influenced to bulk-like dynamics in nanoscopically confined water. *J. Phys. Chem. B* 113:7973–76
122. Liu P, Harder E, Berne BJ. 2004. On the calculation of diffusion coefficients in confined fluids and interfaces with an application to the liquid-vapor interface of water. *J. Phys. Chem. B* 108:6595–602
123. Makarov VA, Feig M, Andrews BK, Pettitt BM. 1998. Diffusion of solvent around biomolecular solutes: a molecular dynamics simulation study. *Biophys. J.* 75:150–58

124. Jana B, Pal S, Bagchi B. 2010. Enhanced tetrahedral ordering of water molecules in minor grooves of DNA: relative role of DNA rigidity, nanoconfinement, and surface specific interactions. *J. Phys. Chem. B* 114:3633–38
125. Sendner C, Horinek D, Bocquet L, Netz RR. 2009. Interfacial water at hydrophobic and hydrophilic surfaces: slip, viscosity, and diffusion. *Langmuir* 25:10768–81
126. Hummer G, Rasaiah JC, Noworyta JP. 2001. Water conduction through the hydrophobic channel of a carbon nanotube. *Nature* 414:188–90
127. Majumder M, Chopra N, Andrews R, Hinds BJ. 2005. Nanoscale hydrodynamics: enhanced flow in carbon nanotubes. *Nature* 438:44
128. Joseph S, Aluru NR. 2008. Why are carbon nanotubes fast transporters of water? *Nano Lett.* 8:452–58
129. Thomas JA, McGaughey AJH. 2008. Reassessing fast water transport through carbon nanotubes. *Nano Lett.* 8:2788–93
130. Cahill DG, Ford WK, Goodson KE, Mahan GD, Majumdar A, et al. 2003. Nanoscale thermal transport. *J. Appl. Phys.* 93:793–818
131. Huang DM, Sendner C, Horinek D, Netz RR, Bocquet L. 2008. Water slippage versus contact angle: a quasiuniversal relationship. *Phys. Rev. Lett.* 101:226101
132. Willard AP, Chandler D. 2009. Coarse-grained modeling of the interface between water and heterogeneous surfaces. *Faraday Discuss.* 141:209–220
133. Kuna JJ, Voitchovsky K, Singh C, Jiang H, Mwenifumbo S, et al. 2009. The effect of nanometre-scale structure on interfacial energy. *Nat. Mater.* 8:837–42
134. Luzar A, Leung K. 2000. Dynamics of capillary evaporation. I. Effect of morphology of hydrophobic surfaces. *J. Chem. Phys.* 113:5836–44
135. Zhou RH, Huang XH, Margulis CJ, Berne BJ. 2004. Hydrophobic collapse in multidomain protein folding. *Science* 305:1605–9
136. Huang XH, Zhou RH, Berne BJ. 2005. Drying and hydrophobic collapse of paraffin plates. *J. Phys. Chem. B* 109:3546–52
137. Giovambattista N, Rossky PJ, Debenedetti PG. 2009. Effect of temperature on the structure and phase behavior of water confined by hydrophobic, hydrophilic, and heterogeneous surfaces. *J. Phys. Chem. B* 113:13723–34
138. Edison JR, Monson PA. 2010. Dynamic mean field theory of condensation and evaporation processes for fluids in porous materials: application to partial drying and drying. *Faraday Discuss.* 146:167–84
139. Yin H, Hummer G, Rasaiah JC. 2007. Metastable water clusters in the nonpolar cavities of the thermostable protein tetrabrachion. *J. Am. Chem. Soc.* 129:7369–77
140. Setny P, Baron R, McCammon JA. 2010. How can hydrophobic association be enthalpy driven? *J. Chem. Theory Comput.* 6:2866–71
141. Baron R, Setny P, McCammon JA. 2010. Water in cavity-ligand recognition. *J. Am. Chem. Soc.* 132:12091–97
142. Setny P, Wang Z, Cheng LT, Li B, McCammon JA, Dzubiella J. 2009. Dewetting-controlled binding of ligands to hydrophobic pockets. *Phys. Rev. Lett.* 103:187801
143. Kalra A, Garde S, Hummer G. 2003. Osmotic water transport through carbon nanotube membranes. *Proc. Natl. Acad. Sci. USA* 100:10175–80
144. Li JY, Gong XJ, Lu HJ, Li D, Fang HP, Zhou RH. 2007. Electrostatic gating of a nanometer water channel. *Proc. Natl. Acad. Sci. USA* 104:3687–92
145. Black SD, Mould DR. 1991. Development of hydrophobicity parameters to analyze proteins which bear posttranslational or cotranslational modifications. *Anal. Biochem.* 193:72–82
146. Kyte J, Doolittle RF. 1982. A simple method for displaying the hydropathic character of a protein. *J. Mol. Biol.* 157:105–32
147. Chennamsetty N, Voynov V, Kayser V, Helk B, Trout BL. 2009. Design of therapeutic proteins with enhanced stability. *Proc. Natl. Acad. Sci. USA* 106:11937–42
148. Siebert X, Hummer G. 2002. Hydrophobicity maps of the N-peptide coiled coil of HIV-1 gp41. *Biochemistry* 41:2956–61

149. Landon MR, Lieberman RL, Hoang QQ, Ju SL, Caaveiro JMM, et al. 2009. Detection of ligand binding hot spots on protein surfaces via fragment-based methods: application to DJ-1 and glucocerebrosidase. *J. Comput.-Aided Mol. Des.* 23:491–500
150. Wong SS, Joselevich E, Woolley AT, Cheung CL, Lieber CM. 1998. Covalently functionalized nanotubes as nanometre-sized probes in chemistry and biology. *Nature* 394:52–55
151. Wong SS, Woolley AT, Joselevich E, Cheung CL, Lieber CM. 1998. Covalently-functionalized single-walled carbon nanotube probe tips for chemical force microscopy. *J. Am. Chem. Soc.* 120:8557–58
152. Morrison CJ, Godawat R, McCallum SA, Garde S, Cramer SM. 2009. Mechanistic studies of displacer-protein binding in chemically selective displacement systems using NMR and MD simulations. *Biotechnol. Bioeng.* 102:1428–37
153. Giovambattista N, Lopez CF, Rossky PJ, Debenedetti PG. 2008. Hydrophobicity of protein surfaces: separating geometry from chemistry. *Proc. Natl. Acad. Sci. USA* 105:2274–79
154. Quere D. 2005. Non-sticking drops. *Rep. Prog. Phys.* 68:2495–532
155. Gao LC, McCarthy TJ. 2007. How Wenzel and Cassie were wrong. *Langmuir* 23:3762–65
156. Gao LC, McCarthy TJ. 2006. The "lotus effect" explained: two reasons why two length scales of topography are important. *Langmuir* 22:2966–67
157. Cassie ABD, Baxter S. 1945. Large contact angles of plant and animal surfaces. *Nature* 155:21–22
158. Wenzel RN. 1936. Resistance of solid surfaces to wetting by water. *Ind. Eng. Chem.* 8:988–94
159. Koishi T, Yasuoka K, Fujikawa S, Ebisuzaki T, Zeng XC. 2009. Coexistence and transition between Cassie and Wenzel state on pillared hydrophobic surface. *Proc. Natl. Acad. Sci. USA* 106:8435–40
160. Grzelak EM, Errington JR. 2010. Nanoscale limit to the applicability of Wenzel's equation. *Langmuir* 26:13297–304
161. Grzelak EM, Shen VK, Errington JR. 2010. Molecular simulation study of anisotropic wetting. *Langmuir* 26:8274–81
162. Mittal J, Hummer G. 2010. Interfacial thermodynamics of confined water near molecularly rough surfaces. *Faraday Discuss.* 146:341–52
163. Daub DC, Wang J, Kudesia S, Bratko D, Luzar A. 2010. The influence of molecular scale roughness on the surface spreading of an aqueous nanodrop. *Faraday Discuss.* 146:67–77
164. Gao LC, McCarthy TJ. 2006. Contact angle hysteresis explained. *Langmuir* 22:6234–37
165. Shirts M, Pande VS. 2000. Computing: screen savers of the world unite! *Science* 290:1903–4
166. LeBard DN, Matyushov DV. 2008. Dynamical transition, hydrophobic interface, and the temperature dependence of electrostatic fluctuations in proteins. *Phys. Rev. E* 78:061901
167. Strong M, Sawaya MR, Wang SS, Phillips M, Cascio D, Eisenberg D. 2006. Toward the structural genomics of complexes: Crystal structure of a pe/ppe protein complex from mycobacterium tuberculosis. *Proc. Natl. Acad. Sci. USA* 103:8060–65
168. Lin EI, Shell MS. 2010. Can peptide folding simulations provide predictive information for aggregation propensity? *J. Phys. Chem. B* 114:11899–908
169. Cellmer T, Bratko D, Prausnitz JM, Blanch HW. 2007. Protein aggregation in silico. *Trends Biotechnol.* 25:254–61
170. Bratko D, Cellmer T, Prausnitz JM, Blanch HW. 2007. Molecular simulation of protein aggregation. *Biotechnol. Bioeng.* 96:1–8
171. Curtis RA, Ulrich J, Montaser A, Prausnitz JM, Blanch HW. 2002. Protein-protein interactions in concentrated electrolyte solutions—Hofmeister-series effects. *Biotechnol. Bioeng.* 79:367–80
172. Hoyer W, Gronwall C, Jonsson A, Stahl S, Hard T. 2008. Stabilization of a β-hairpin in monomeric Alzheimer's amyloid-β peptide inhibits amyloid formation. *Proc. Natl. Acad. Sci. USA* 105:5099–104
173. Hummer G, Garde S, Garcia AE, Pratt LR. 2000. New perspectives on hydrophobic effects. *Chem. Phys.* 258:349–70
174. Lipman EA, Schuler B, Bakajin O, Eaton WA. 2003. Single-molecule measurement of protein folding kinetics. *Science* 301:1233–35
175. Dzubiella J. 2007. Interface dynamics of microscopic cavities in water. *J. Chem. Phys.* 126:194504
176. Marrink SJ, Risselada HJ, Yefimov S, Tieleman DP, de Vries AH. 2007. The Martini force field: coarse grained model for biomolecular simulations. *J. Phys. Chem. B* 111:7812–24

177. Shinoda W, Devane R, Klein ML. 2007. Multi-property fitting and parameterization of a coarse grained model for aqueous surfactants. *Mol. Simul.* 33:27–36
178. Izvekov S, Voth GA. 2005. A multiscale coarse-graining method for biomolecular systems. *J. Phys. Chem. B* 109:2469–73
179. Baoukina S, Monticelli L, Risselada HJ, Marrink SJ, Tieleman DP. 2008. The molecular mechanism of lipid monolayer collapse. *Proc. Natl. Acad. Sci. USA* 105:10803–8
180. Wong-Ekkabut J, Baoukina S, Triampo W, Tang IM, Tieleman DP, Monticelli L. 2008. Computer simulation study of fullerene translocation through lipid membranes. *Nat. Nanotechnol.* 3:363–68
181. Weeks JD, Katsov K, Vollmayr K. 1998. Roles of repulsive and attractive forces in determining the structure of nonuniform liquids: generalized mean field theory. *Phys. Rev. Lett.* 81:4400–3
182. Rodgers JM, Weeks JD. 2008. Interplay of local hydrogen-bonding and long-ranged dipolar forces in simulations of confined water. *Proc. Natl. Acad. Sci. USA* 105:19136–41
183. Rodgers JM, Weeks JD. 2009. Accurate thermodynamics for short-ranged truncations of coulomb interactions in site-site molecular models. *J. Chem. Phys.* 131:244108
184. Berendsen HJC, Vanderspoel D, Vandrunen R. 1995. Gromacs—a message-passing parallel molecular-dynamics implementation. *Comput. Phys. Commun.* 91:43–56
185. Lindahl E, Hess B, Van Der Spoel D. 2001. Gromacs 3.0: a package for molecular simulation and trajectory analysis. *J. Mol. Model.* 7:306–17
186. Phillips JC, Braun R, Wang W, Gumbart J, Tajkhorshid E, et al. 2005. Scalable molecular dynamics with NAMD. *J. Comput. Chem.* 26:1781–802

Annual Review of Chemical and Biomolecular Engineering

Volume 2, 2011

Contents